Dynamic Strain Aging and the Bauschinger Effect During Cyclic Deformation in Polycrystalline Silver and Copper Base Solid Solutional Alloys

By

Satoshi HASHIMOTO* and Sei MIURA*

(Received June 27, 1985)

Abstract

In order to investigate the characteristics of the P-L effect and to obtain additional information on the production of vacancies during tensile and fatigue deformation, tensile and tension-compression tests were performed in Ag-6.3 at.% Al and α-brass polycrystals. It was found that the P-L effect in Ag-Al alloy is well explained by the dynamic strain aging model by Cottrell. The effective activation energy for the migration of a vacancy in Ag-Al alloy is estimated to be 0.6 ± 0.02 eV. It was also confirmed, from the experiment of annealing the excess vacancies, that the P-L effect is strongly affected by the accumulation of vacancies produced by strain. The strain exponent m, of a vacancy concentration produced by strain, was determined to be $m=1.35$. This is equal to that obtained from the static strain aging experiment, assuming the strain exponent of total dislocation density to be $\beta=1$. In the cyclic straining conducted under the prescribed strain amplitude, the cumulative strain to the onset of the P-L effect is greater for a lower strain amplitude. However, the values subtracted by the sum of a Bauschinger strain β_1 in each half cycle from the cumulative strains give an approximately constant value independent of the magnitude of the strain amplitude. The values are larger than the critical strain for the onset of the P-L effect in unidirectional deformation by an amount of 20% in both alloys. From the results, it can be concluded that vacancies are produced only in the complete plastic strain region subsequent to the Bauschinger strain β_1 during cyclic straining. Hence, the efficiency of the vacancy production would decrease with an increase in the number of cycles. Namely, the saturation of the vacancy production is to be directly correlated to the saturation of the cyclic strain hardening. Furthermore, it is suggested that the efficiency of the vacancy production during the cyclic straining is lower by 20%, even in the complete plastic strain region, probably because of the vacancy-interstitial annililation.

1. Introduction

Within certain combinations of temperature and strain rate, serrated yielding (serration) is observed in both substitutional and interstitial solid solutional alloys.

* Department of Engineering Science, Faculty of Engineering, Kyoto University, Kyoto-606 Japan

This phenomenon, which is generally referred to as the Portevin-Le Chatelier (P-L) effect, named after the original investigators of this phenomenon in aluminium alloys[1], has received considerable attention in resent years[2,3]. In substitutional alloys, this phenomenon is generally attributed to the interaction between moving dislocations and solute atoms enhanced by non-equilibrium vacancies produced by deformation or dynamic strain aging. It is also well recognized that dynamic strain aging is manifested by an increase in flow stress, a negative temperature and a strain-rate dependence of the flow stress as well as a reduction of ductility, compared with the values or tendencies expected in the absence of the strain aging effect[4-6].

The manifestation of the P-L effect on the development of a dislocation substructure and the solute atmosphere in cyclic deformation is of considerable interest, since strain aging plays an important role in the improvement of the fatigue strength. The fact that strain aging can enhance the fatigue strength of ferritic steels is well established[7,8]. The manner in which it operates during continuous cycling has been investigated from the view point of crack growth in low-carbon steel[9-12]. However, the features of the P-L effect during cyclic deformation, especially low cycle fatigue deformation, is not well documented, although some work on the effect of dynamic strain aging on reverse straining or cyclic straining has been reported[13-16].

It has long been considered that a reverse deformation may create vacancies at a rate greater than unidirectional deformation. Some experimental evidence to show that large concentrations of point defects may accummulate during fatigue have been reported[17,18]. In recent years, resistivity measurements on fatigued metals have again attracted significant attention by many investigators. More precise information on the production of point defects during fatigue in pure fcc metals has been described. The purpose of the present work is to investigate the characteristics of the P-L effect during tensile deformation in Ag-Al polycrystals, from the view point of strain-induced vacancies for promoting the effect as well as the features of the appearance of the effect during the early stage of cyclic straining of polycrystalline Ag-Al and α-brass alloys. In addition, the efficiency of vacancy production during the course of cyclic straining is discussed, compared with the nature of the P-L effect in tensile deformation. The significant role of the Bauschinger effect during cyclic deformation, when considering the manifestation of the P-L effect and the process of point defect production during fatigue deformation, is also considered.

2. Experimental Procedures

The materials used in this investigation were Ag-6.3 at.% Al, prepared from 99.99% Ag and 99.99 % Al, and α-brass (69.08 wt.% Cu, 0.001 wt.% Fe, Pb,

remainder Zn). Tensile specimens of Ag-Al were obtained from wires of 1.4 mm in diameter, and 70 mm in length, by cutting. The specimens were initially straightened after annealing at 500°C for 10 minutes in vacuo, and then annealed at 700°C and 800°C for 2 hours and furnace cooled to room temperature. The grain diameter was 185 μm and 310 μm respectively.

Tension-compression specimens of both Ag-Al and α-brass alloys were machined from 6 mm in diameter rods. The resulting dimensions of the specimens were 3.0-3.5 mm in diameter and 8.0 mm in gauge length. Both alloy specimens were annealed at 800°C for 2 hours in vacuo, and the grain diameters obtained werea bout 250 μm and 100 μm, respectively.

The Instron type testing machine was used for the tensile test. Gauge lengths of the specimen were fixed at 50 mm. The strain rate employed ranged from 3.3×10^{-5} to 4×10^{-3}/sec. The deformation temperatures were controlled by using a water bath or a methyl alcohol bath refrigerated by liquid nitrogen. For the tension-compression test, the specimen shoulders were soldered into grips, and were strained in a specially designed push-pull jig equipped in the testing machine. Load-elongation curves were automatically recorded by applying a LVDT extensometer fitted on the specimen shoulders and load cell out-puts to an X-Y recorder. The deformation temperature ranged from 20 to 45°C for Ag-Al, but mainly 80°C for α-brass, using a water bath or a silicon oil bath when necessary. The strain rate employed was mainly 5×10^{-4}/sec. These conditions can give rise to the onset of serration after several per cent of smooth curve in the tensile deformation of both alloys.

3. Theoretical Basis on Strain Aging

3.1. Dynamic strain aging (The Portevin-Le Chatelier effect)

A theory for the P-L effect is based on the interaction between solute atoms and dislocations at temperatures where serrated yielding begins when the velocity of dislocations equals the drift velocity of solute atoms in the stress field of dislocation. This model is the dynamic strain aging model of Cottrell[19,20], but subsequently modified by further investigators[4,6,21,22].

The velocity of the moving solute atom V_i is given by the Einstein relation[23] as

$$V_i=\frac{DF}{kT} \tag{1}$$

where F is the interaction force between the dislocation and solute atom, k is Boltzmann's constant and T is the temperature's degree in Kelvin. For substitutional alloys, the diffusion coeficient D is given by Seitz[24] and Mott[25] as

$$D=a^2\nu ZC_v\exp(-E_m/kT), \tag{2}$$

where a is the lattice parameter, ν the Debye frequency, Z the coordinatation num-

ber (12 for fcc substitutional alloy), C_v the vacancy concentration and E_m the effective activation energy for the exchange of a vacancy and a solute atom. The mean velocity of dislocation V_d is represented in terms of the strain rate $\dot{\varepsilon}$, and the mobile dislocation density ρ_m as

$$V_d=\dot{\varepsilon}/b\rho_m, \tag{3}$$

where b is the Burgers vector.

The total vacancy concentration C_v strictly depends on three factors: (i) the con centration of thermal vacancies at the test temperature, C_v^T; (ii) the productions of excess vacancies during plastic straining, C_v^ε; and (iii) the annihilation of vacancies at sinks during straining, C_v^-. The value of C_v is therefore given by

$$C_v=C_v^T+C_v^\varepsilon-C_v^-. \tag{4}$$

In practice, however, use of this equation (4) leads to a complicated expression[26,27], and it is usually assumed that C_v^T and C_v^- are negligibly small when compared with C_v^ε. For example, under the condition of $T=293$°K and $\varepsilon=0.1$, $C_v^T\approx10^{-12}$ and $C_v\approx10^{-5}$. The annihilation of vacancies during straining, C_v^-, becomes important at high temperatures and low strain rates, and leads to derivations from the model which have been observed experimentally in an Al-Mg alloy[26,28]. However, it will be demonstrated in this work that at relativey lower temperatures of these experiments, the results are in good agreement with the model, assuming that, $C_v^-\ll C_v^\varepsilon$. Therefore, it is reasonable to postulate that $C_v\simeq C_v^\varepsilon$. The concentration of strain-induced vacancies, C_v, may be expressed by[29]

$$C_v=B\varepsilon^m, \tag{5}$$

where B and m are constants and ε the plastic strain. (From now on, C_v^ε will be referred to as the C_v). Theoretical estimates[24,25,30,31] and resistivity measurements[32] give $m\simeq1$-1.5 and $B\simeq10^{-4}$.

The mobile dislocation density with strain, ρ_m, may either increase or remain constant during straining, but unfortunately the precise dependence is not known. However, experiments show that at low strains the total dislocation density, ρ_t, increases essentially linearly with strain[22,33], so that, by assuming ρ_m is a constant fraction of ρ_t, it is possible to express ρ_m as[22]

$$\rho_m=f\rho_t=fN\varepsilon^\beta, \tag{6 a, b}$$

where f, N and β are constants, and for many metals $N\simeq10^{11}$ and $\beta\simeq1$.

Next, considering the onset of the P-L effect, from the above hypothesis $V_i\simeq V_d$, the relation between the critical strain for the onset of serration, ε_o, strain rate, $\dot{\varepsilon}$ and deformation temperature, T can be expressed as

$$\dot{\varepsilon}T=(\text{const})\rho_m C_v\exp(-E_m/kT)$$
$$\dot{\varepsilon}T\propto\varepsilon_o{}^{m+\beta}\exp(-E_m/kT). \tag{7 a, b}$$

At a given temperature, the relation between $\dot{\varepsilon}$ and ε_o is expressed as

$$\log \dot{\varepsilon} \propto (m+\beta) \log \varepsilon_o. \tag{8}$$

As the values of $(m+\beta)$ are nearly equal to each other at various temperatures (to be shown later), when ε_o is constant in Eq. (7), the activation energy E_m, is calculated from the relation as

$$\log \dot{\varepsilon} T \propto (-E_m/k)(1/T). \tag{9}$$

3.2. Static strain aging

Cottrell and Bilby[34] have shown that, in a strain aging process, the fraction of total dissolved solute (n_t/n_o) migrating to dislocations in time t at temperature T may be written:

$$n_t/n_o = \alpha \rho_t \left(\frac{ADt}{kT}\right)^{2/3}, \tag{10}$$

where n_o is the number of atoms originally in solid solution, A an elastic parameter concerned with the interaction between solute atoms and dislocations, ρ_t the total dislocation density and α a constant. Harper[35] has modified this law to take into account the depletion of the bulk by segregation. If a maximum number, n, of solute atoms segregate, the fraction segregated, $f=n_t/n$, may be defined, assuming that the rate of segregation is proportional to the fraction unsegregated[36],

$$\frac{\partial f}{\partial t} = (1-f)\phi(t), \tag{11}$$

where $\phi(t)$ is a function to be determined. This may be solved under the condition that the equation of Cottrell and Bilby, which applies only to short periods, is observed. A relation similar to Harper's is derived[36], namely,

$$f = 1 - \exp\left[-\frac{\alpha n_o}{n}\rho_t \left(\frac{ADt}{kT}\right)^{2/3}\right]. \tag{12}$$

In order to use this relation, it must now be assumed that $\Delta\sigma$, the increase in flow stress at time t, is proportional to n_t, and it follows that

$$\gamma(n_t/n) = \frac{\Delta\sigma}{\Delta\sigma_{\max}} = f, \tag{13}$$

where γ is a proportionality constant which allows for the incomplete segregation of available solute to dislocations at the end of aging. It must also be assumed that n is independent of temperature in the range considered. Consequently, the relation can be obtained as

$$1-f = \exp\left[-(\text{const})\rho_t \left(\frac{ADt}{kT}\right)^p\right]. \tag{14}$$

The time exponent p is 2/3 in the theory. However, for a long aging time it reaches a value between 1/3 and 1/2 [37,38].

By substituting Eqs. (2) and (6) in Eq. (14),

$$1-f = \exp[-(\text{const})\varepsilon^{pm+\beta}\{\exp(-E_m/kT)t/kT\}^p]. \tag{15}$$

At a given strain ε and temperature T,

$$\log\log(1-f) \propto p \log t. \tag{16}$$

Also at a given f and T,

$$t \propto \varepsilon^{-(m+\frac{1}{p}\beta)}. \tag{17}$$

Hence, the time exponent p and $(m+\frac{1}{p}\beta)$ can be determined by the plots in accord with these above equations.

4. Results and Discussion

4.1. The P-L effect in tensile deformation of Ag-6.3 at.% Al polycrystals

4.1.1. Effect of strain rate and temperature on the onset of serration

Here, the results are only concerned with the so-called type A serration which appears at relatively low temperatures. A typical stress-strain curve in which serrated yielding is observed is shown in Fig. 1. In the figure, the critical strain ε_0 for the onset of serration is also indicated. The strain rate $\dot{\varepsilon}$ dependence of the strain to the onset of serrations ε_0 is shown in Fig. 2. These plots yield single straight lines, and also give an approximately constant value of $m+\beta=2.44$ at various deformation temperatures for the specimen annealed at 700°C, $m+\beta=2.50$ for that annealed at 800°C. This validates that the relation (8) is well established.

The relationships between critical strain for the onset of serration, deformation temperature and strain rate are shown in Fig. 3.

4.1.2. Activation energy for migration of a vacancy

Since the values of $(m+\beta)$ are constant in the temperature range of 30-80°C,

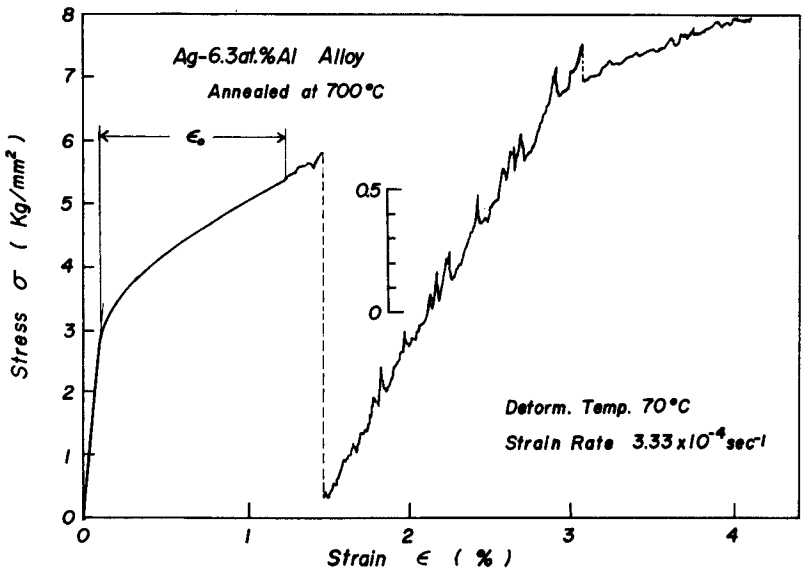

Fig. 1. Typical stress-strain curve showing the P-L effect in Ag-6.3 at.% Al alloy. ε_0 is the plastic strain at which the first serration occurs. Part of the curve was magnified.

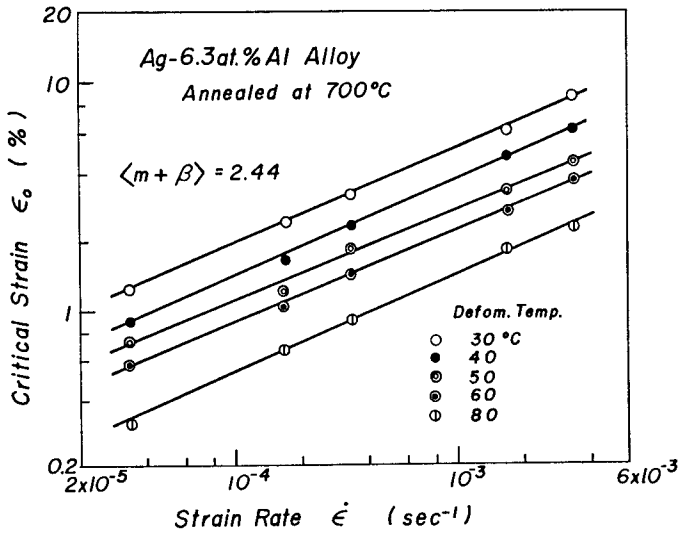

Fig. 2. Relation between critical strain and strain rate for selected deformation temperatures in Ag-6.3 at.% Al alloy. The slope of the line gives the value of $m+\beta$.

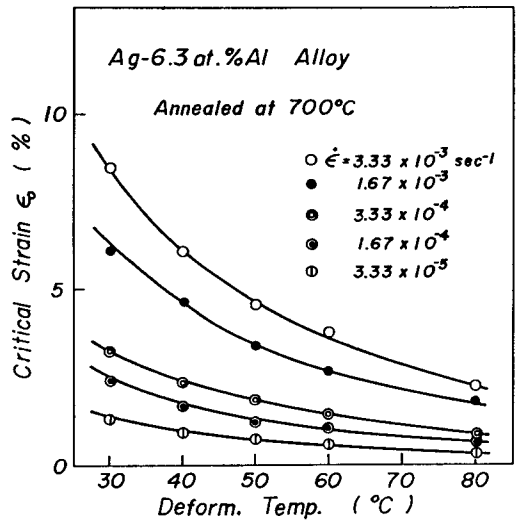

Fig. 3. Relation between critical strain and the deformation temperature for selected strain rates.

as shown in Fig. 2, the activation energy for the migration of a vacancy can be determined experimentally from the relation of Eq. (9) by $\log \dot{\varepsilon}(T)$ vs $1/T$ plots. Figure 4 shows these plots at three selected strains, giving the value of $E_m = 0.60 \pm 0.02$ eV for the larger grain size and of $E_m = 0.63 \pm 0.02$ eV for the smaller one.

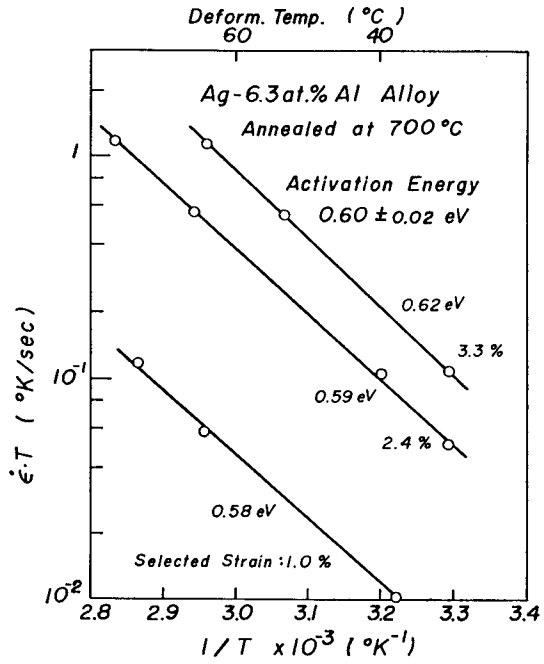

Fig. 4. Relation between strain rate and temperature for determining activation energy for the process.

The activation energy for the migration of a vacancy in pure silver is usually reported as 0.83-0.88 eV[39-41] from the quench experiment. Dawson[42] has reported, from the resistivity measurements of the recovery process of Stage IV after various degrees of plastic deformation, that this stage is explained by the migration of a single vacancy, and the activation energy is estimated to be 0.89 ± 0.03 eV. In general, if a vacancy migrates by breaking away from a solute atom, the activation energy for migration of a vacancy is shown as $E_{IV}^m + E^B$, where E_{IV}^m is the activation energy for the migration of a vacancy in pure metal and E^B the binding energy between a vacancy and a solute atom. But, if a vacancy and a solute atom migrate togather as a vacancy-solute atom complex, the activation energy for a pair of vacancy-solute atoms may be given by $E_{IV}^m - E^B$[20]. From the activation energy obtained in this experiment, it is therefore considered that a vacancy migrates as a vacancy-solute atom complex at the temperatures employed in this alloy. Adopting 0.86 eV as a migration energy of a vacancy in pure silver, the binding energy E^B is estimated to be $E^B = 0.86 - (0.60 - 0.63) = 0.26 - 0.23$ eV. At present, the binding energy between a vacancy and a solute atom in silver alloy is not well established. Only Quere[43] has reported that $E^B = 0.35$ eV for Ag-O alloy. Cattaneo and Germagnoli[44] have reported that $E^B = 0.3$ eV for Au-0.1% Ag alloy. Although it is difficult to

determine the value of E^B from the present results, the value obtained is considered to be reasonable.

Hendrickson and Fine[37] found that E_m is 0.41 eV for the early stage of aging, and 0.55 eV for the later stage. They suggested that the low initial activation energies are due to the motion of atom-vacancy complexes, and that the later time activation energy may be associated with the motion of atom-single vacancy pairs. The migration energy for di-vacancies in pure silver was reported to be 0.57-0.58 eV[41,43,45]. Di-vacancies will be created by the plastic deformation of silver, but the concentration may be smaller than that of a single vacancy. Furthermore, Dawson[42] has reported, from the results of resistivity isochronals of silver after the deformation less than 10% strain, that Stage IV started at 50°C. Therefore, it is reasonable to conclude that single vacancy-solute atom pairs migrate at the temperatures employed in this alloy.

4.2. Vacancies induced by unidirectinal plastic strain

4.2.1. Effect of vacancy annealing on the onset of serration

It is considered that the excess vacancies created by plastic strain play a very important role in initiating the P-L effect in this alloy. If a specimen is pre-strained to ε_p, and then arrested, the resulting accumulation of vacancies will be annealed out, while the accumulation of dislocations will not, the first serrated yielding will be delayed. When the deformation is resumed at the same strain rate and temperature, serration will occur at the total strain (including the pre-strain) $\varepsilon_t > \varepsilon_o$, when $C_v = B(\varepsilon_t{}^m - \varepsilon_p{}^m)$ and $\rho_m = fN\varepsilon_t$. Equation (7a) shows that when $\rho_m C_v$ reaches a certain value, the P-L effect starts. Thus, for the pre-strain experiment, the following relation is obtained as[22]

$$\varepsilon_o{}^{m+\beta} = \varepsilon_t{}^{\beta}(\varepsilon_t{}^m - \varepsilon_p{}^m) \tag{18}$$

Hence, the vacancy concentration index m is determined by[46]

$$m = \frac{\log\{1-(\varepsilon_o/\varepsilon_t)^{m+\beta}\}}{\log(\varepsilon_p/\varepsilon_t)}. \tag{19}$$

Dawson[42] has reported that after several per cent of plastic strain, the temperature range where single vacancy migrates is about 30-60°C, and Stage V due to the recovery of dislocations is not observed even at 100°C from the results of resistivity isochronals of silver. Therefore, the experiment was carried out at a strain rate of 3.3×10^{-4}/sec, and 20°C; the vacancy annealing was conducted usually at 99°C. The specimens were given different tensile pre-strains, rested 10-40 minutes at those temperatures, and then the tensile strain to the first serration was measured. After the vacancy annealing treatment, decreases in flow stress were not found in any of the specimens tested. Hence, it is considered that no recovery of dislocations occurs by the treatment. The results for the specimens annealed at 700°C and 800°C are shown in Table 1. A specimen was pre-strained and annealed at 20°C for 10

Table 1. Effect of pre-strain upon the total-strain to the onset of serration in specimen annealed at 700°C and 800°C. (Deformation temperature 20°C, strain rate 3.33×10^{-4}/sec.)

	Annealing Temp. (°C)	Annealing Time(min)	Pre-strain ε_p (%)	Total-strain ε_t (%)	m	β
700	—	—	—	4.10		
	—	—	—	4.14		
	20	10	0.98	4.10		$m+\beta=2.44$
				$\bar{\varepsilon}_0=4.11$		
	55	25	1.92	4.68	1.46	
	99	10	2.10	4.74	1.51	
	99	20	2.62	5.28	1.14	$m=1.3\pm0.2$
	99	40	2.90	5.30	1.28	$\beta=1.14$
800	—	—	—	4.62		
	—	—	—	4.46		
	—	—	—	4.78		$m+\beta=2.50$
				$\bar{\varepsilon}_0=4.62$		
	99	10	1.55	4.99	1.49	
	99	10	2.10	5.34	1.27	
	99	10	2.94	5.82	1.21	$m=1.35\pm0.15$
	99	10	2.94	5.82	1.21	$\beta=1.15$

minutes, but the measured total strain to the onset of serration was equal to the critical strain ε_0, as shown in the table. This indicates that the life time of vacancies at 20°C is larger than the order of 10 minutes. It is seen that as pre-strain increases, the total strain to the onset of serration increases. The results give average values of $m=1.32$ and so $\beta=1.15$, as compared to the values of $m=1.03$ and $\beta=1.17$ reported by Ham and Jaffrey[22] for Cu-Sn alloy and of $m=1.19$ and $\beta=0.95$ by Soler-Gomez and McG. Tegart[46] for Au-In alloy. The value of β, when m is subtracted from $(m+\beta)$, is the value of the exponent for mobile dislocation density, assuming that the constant fraction, f in Eq. (6), is independent of strain.

4.2.2. Estimation of m by the static strain aging experiment

The static strain aging experiment was performed in order to obtain information concerning the creation of vacancies and the accummulation of dislocations produced by plastic strain. In this test, specimens annealed at 700°C were used. The specimens were deformed at a constant strain rate of 1.67×10^{-3}/sec to a specific strain. Straining was discontinued and the specimen was aged for a fixed time t, under the applied stress. The tensile machine was restarted and the straining continued to a second specific strain, and the process was repeated, using the same aging time. The selected aging times and aging temperature were 60, 300, 1200

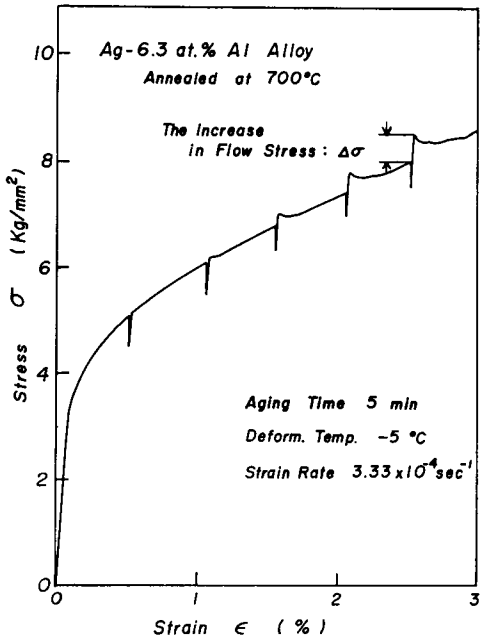

Fig. 5. Typical stress-strain curve showing static strain aging.

seconds and 18°C, respectively.

The increase in flow stress due to the static strain aging and the stress-strain curve is shown in Fig. 5, which serves to indicate the testing procedure and measurements made. The effects of the strain and aging time on the increase in flow stress, $\Delta\sigma$, are shown in Fig. 6. The upper limit of the range is determined by the interference of the onset of serrated yielding which caused scatter in the results. The maximum increase in the flow stress, $\Delta\sigma_{max}$ was estimated to be 0.70 kg/mm², since it is assumed that the same maximum increase was reached at lower tenperatures, that the aging time was sufficiently long[47].

Based on the relation (16), $-\log(1-f)$ against aging time was plotted on a log vs. log scale. The values of the time exponent p at constant plastic strain of 5, 7 and 9% were determined from the slopes, as shown in Fig. 7. The estimated average value of p was 0.39, as compared with the value of $p\simeq 0.4$ reported by Miura and Kawano[38] for more than 10 sec in aging time in Al-Mg alloy. Next, the log of the time required to reach a given value of f was plotted against the log of the plastic strain, based on the relation (17), as shown in Fig. 8. The mean value of $m+\frac{1}{p}\beta$ derived from these slopes was $m+\frac{1}{p}\beta=3.9$. Previously, Bolling[36] and Russell and Vella[47] reported that the slope of the plots gives the value of m, without taking into account the accumulation of dislocations by plastic strain. Thus, the evaluation of m on their stand points must be overestimated.

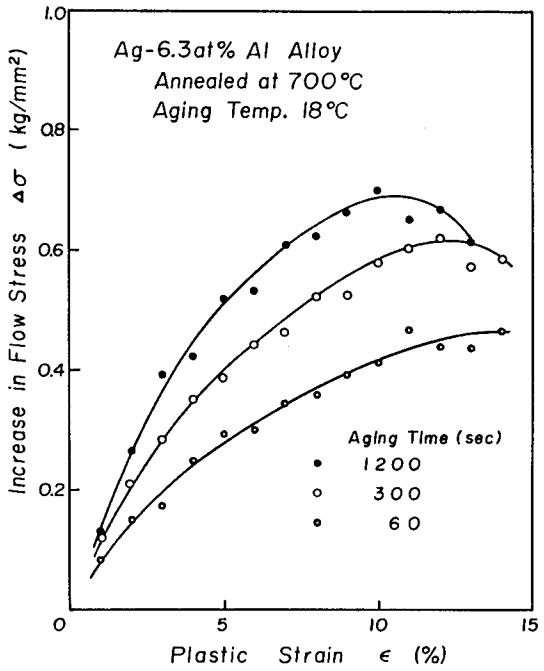

Fig. 6. Relation between the increase in flow stress and aging time.

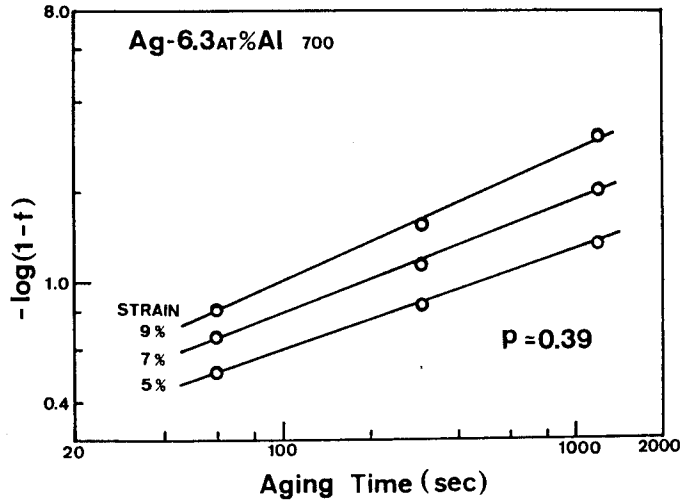

Fig. 7. Relation between $-\log(1-f)$ and aging time for determining the time exponent p in Eq. (14).

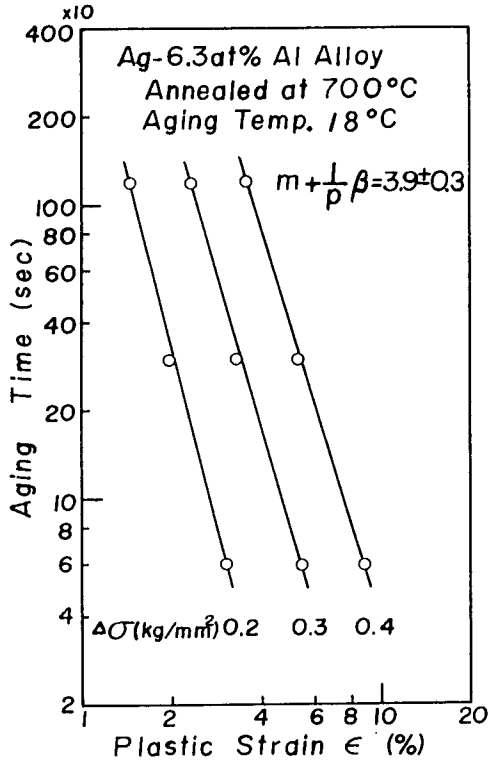

Fig. 8. Relation between the time required to reach a given value of $\Delta\sigma$ and plastic strain for determining the value of $m+\frac{1}{p}\beta$, cf, Eq. (17).

From these results, one can evaluate the value of m by the aid of the knowledge about the value of β. Fortunately, the value of $\beta\simeq1$ has been verified experimentally for a number of metals and alloys[48-50]. From the values of $p=0.39$, $m+\frac{1}{p}\beta=3.9$ and $\beta=1$, the value of m is estimated to be 1.33. This result is in very close agreement with the evaluation of m from the pre-strain experiment of the P-L effect, as indicated in the previous Section 4.2.1.

4.2.3. Effect of vacancy annealing on the static strain aging

In order to confirm the effect of vacancies created by strain on the increase in the flow stress $\Delta\sigma$ due to static strain aging, the following test has been performed. The specimens were deformed by intervals of about 0.5% strain, and aged for 5 minutes at the deformation temperature of -5°C. After pre-straining by ε_s, the specimens were annealed at 90°C for 10 minutes in order to anneal out vacancies created by ε_s, and resumed at the same deformation conditions.

The increase in the flow stress, $\Delta\sigma$, against strain were plotted for three specimens subjected to different pre-strains, ε_s and for that subjected to non-annealing

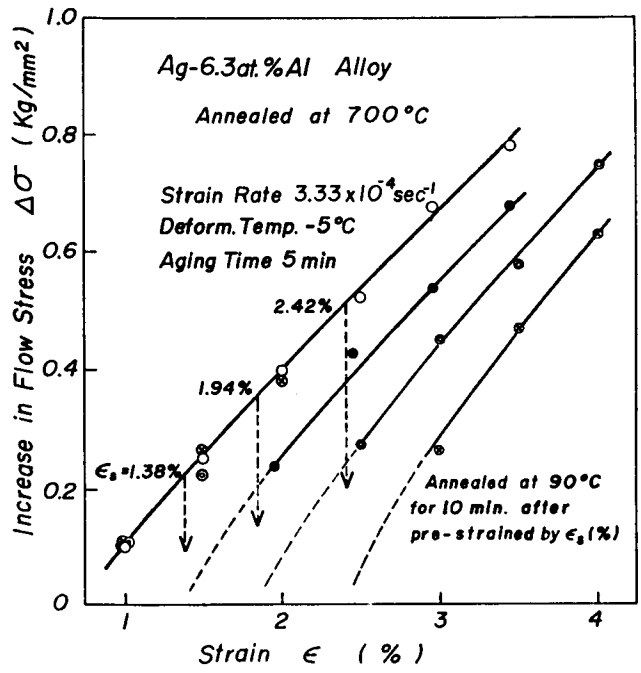

Fig. 9. Effect of vacancy annealing at various amounts of pre-strain on the increase in flow stress due to static strain aging.

treatment, as shown in Fig. 9. As can be clearly seen in the figure, the significant decrease of $\Delta\sigma$ is found after the annealing out of vacancies. The increase in the flow stress $\Delta\sigma$ due to static strain aging must approach zero, if all of the vacancies created by ε_s were annealed out. This was confirmed, since the interpolation of $\Delta\sigma$ to ε_s approached zero for each specimen, as can be indicated by the dotted line in Fig. 9. The results are sufficient evidence for the fact that the increase in flow stress due to static strain aging is controlled by the concentration of vacancies created by the plastic strain in this alloy.

4. 3. Characteristics of the P-L effect in cyclic deformation

In this section, the results are concerned with those of both α-brass and Ag-Al alloy. Detailed investigations on the P-L effect in tensile deformation of α-brass polycrystals and single crystals have been reported elsewhere by Miura and his colleagues[51,52]. Experiments of the effect of the annealing out of vacancies on the P-L effect were also done, in which the effect of annealing on the delay of the onset of serration was established. Then, the strain exponents m and β for the production of vacancies and mobile dislocation density were estimated to be $m=1.5$ and $\beta=1.0$, respectively. Therefore, the values of m for α-brass will be applied in a later analysis of vacancy production by strain.

4. 3. 1. Effect of reverse strain on the onset of serration

In substitutional alloys, it is possible to obtain a smooth curve or a critical amount of strain ε_o before the onset of serration. ε_o is strongly affected by both the accumulation of vacancies created by strain and mobile dislocation density, as mentioned above in the previous Section 4. 2. Periodic serration, yielding the so-called "Type A", was observed after a critical strain $\varepsilon_o=5.82\%$ for tensile deformation with a strain of 5.2×10^{-4}/sec at 80°C in α-brass polycrystal.

Ham and Jaffrey[22] firstly pointed out from the measurement of the start of the P-L effect during reverse straining, that the reverse strain does not create vacancies at a rate greater than unidirectional deformation. But in their paper, the relation between the onset of serration and stress-strain response has not yet been mentioned. Thus, as preliminary experiments, specimens were pre-strained in a tensile direction to strains smaller than ε_o. Then, they were strained further in compression to the extent somewhat past the first serration and the correlation between pre-strain, the reverse strain to the onset of serration and the Bauschinger strain was measured, as shown in Fig. 10. schematically. The results are shown in Table 2.

It is seen the that as the pre-strains ε_p increase, the absolute total strains to the first serration, $\Sigma|\varepsilon|_o=\varepsilon_p+\varepsilon_r$ increase, which are greater than ε_o for unidirectional deformation. The difference between these values is found to be nearly equal to the Bauschinger strain β_1 for the various pre-strains, as shown in terms of $\Sigma|\varepsilon|_o$

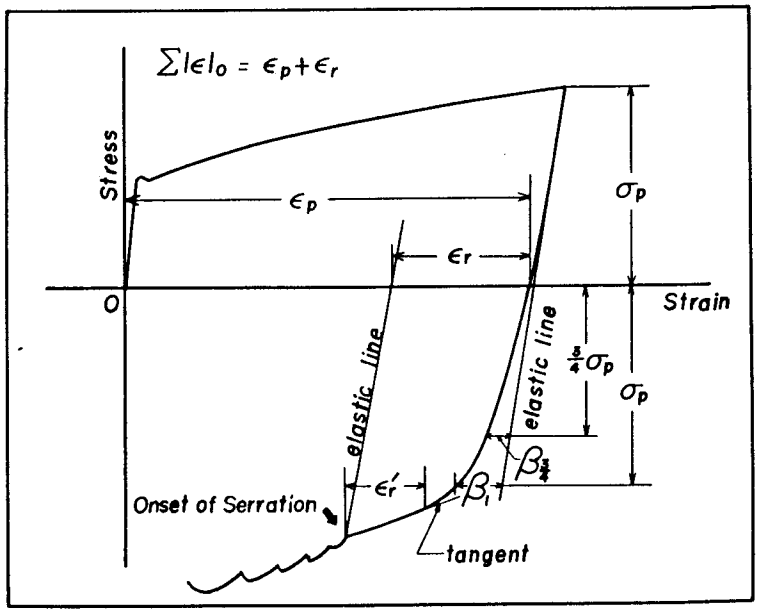

Fig. 10. Schematic reverse stress-strain curve.

Table 2. Effect of reverse straining upon the critical strain for the onset of serration in α-brass.

Specimen No.	ε_p (%)	ε_r (%)	β_1 (%)	$\Sigma\|\varepsilon\|_0$ (%)	$\Sigma\|\varepsilon\|_0-\beta_1$(%)	σ_0(kg/mm^2)
#1005	4.60	1.78	0.70	6.38	5.68	9.99
#1003	4.96	1.87	0.77	6.83	6.05	10.48
#1012	5.45	1.35	0.92	6.80	5.88	10.65

Mean critical strain in tensile deformation, $\varepsilon_0=5.82\%$; and critical stress, $\sigma_0=10.42$ kg/mm^2.

$-\beta_1$. From these results, it appears that the Bauschinger strain region does not play an important role for the start of the P-L effect during reverse straining. The critical stress for the start of serration is also indicated in the table. The critical stress during the reverse straining was approximetely equal to the value in tensile deformation.

4.3.2. Effect of cyclic pre-stressing on the onset of serration

The present test was undertaken to compare the efficiency of vacancy production during unidirectional deformation with that of cyclic deformation. It was done by measuring a critical strain for the onset of serration when a specimen was stressed cyclically before the occurring serrated flow, and then tensile deformation was resumed.

The concentration of vacancies C_v is related to the plastic strain by the relation of Eq. (5). The constants B and m will be different for unidirectional and cyclic deformation, so that for the concentration of vacancies produced by cyclic stressing concerning this experiment, an analogous relation to Eq. (5) is expressed by Dawson[53] as

$$C_{v_f}=B_f(\Sigma\Delta\varepsilon)^{m_f}, \tag{20}$$

where $\Delta\varepsilon$ is the loop width in each cycle, which decreases with an increase in the number of cycles; $\Sigma\Delta\varepsilon$ is the cumulative plastic strain produced by the cyclic stressing, and suffix f is used especially to characterize the fatigue deformation.

If a specimen is pre-strained and then stressed cyclically at the pre-stress amplitude, the resulting accumulation of vacancies will increase, while the accumulation of dislocations will not. When tensile deformation is resumed, the first serration will occur at a total strain (including the pre-strain) $\varepsilon_t>\varepsilon_0$, where $C_v=B\varepsilon_t^m+B_f(\Sigma\Delta\varepsilon)^{m_f}$ and $\rho=fN\varepsilon_t^\beta$. Therefore, when the first serration occurs, one can obtain a relation between unidirectional and cyclic deformation as

$$B\varepsilon_0^{m+\beta}=\varepsilon_t^\beta\{B\varepsilon_t^m+B_f(\Sigma\Delta\varepsilon)^{m_f}\}, \tag{21a}$$

and we finally have logarithmically

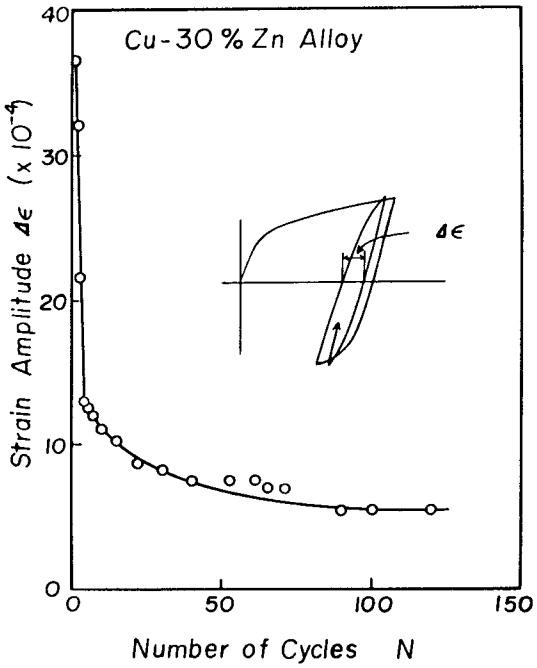

Fig. 11. Variation of strain amplitude (loop width) $\Delta\varepsilon$ during cyclic stressing at the pre-stress amplitude.

Table 3. Effect of cyclic stressing upon the critical strain for the onset of serration.

Number of cycles N	Cumulative strain $\Sigma\Delta\varepsilon$ (%)	Total tensile strain ε_t (%)
500	57.7	5.56
700	78.1	5.36
1000	108.7	4.96
1500	159.7	4.72
2000	210.7	3.88
Critical strain in unidirectional deformation, $\varepsilon_0=5.82\%$		

$$\log\left(\frac{\varepsilon_0^{m+\beta}-\varepsilon_t^{m+\beta}}{\varepsilon_t^{\beta}}\right)=\log\frac{B_f}{B}+m_f\log(\Sigma\Delta\varepsilon). \tag{21b}$$

The present experiment tests this relation.

The specimens were deformed in a water bath maintained at 80±1°C, and the strain rate employed was 5.2×10^{-4}/sec in tensile deformation and 5.2×10^{-3}/sec in cyclic deformation to reduce the time needed to carry out the cyclic stressing. The specimens were pre-strained to 2.0% and then cyclic-stressed at the pre-stress amplitude, so that the loop width $\Delta\varepsilon$ decreased with an increase in the number of

cycles. The results obtained are shown in Fig. 11. By increasing the number of cycles, the total tensile strain ε_t decreased, and the results are shown in Table 3. The values of cumulative strain $\Sigma\Delta\varepsilon$ were taken from an account of a variation of $\Delta\varepsilon$ up to the saturated value as shown in Fig. 11.

If some vacancies were lost during the cyclic deformation, Eqs. (21a, b) could not be established. Therefore, it is important to obtain a knowledge of the life time of vacancies. When the specimens were pre-strained by 2.0%, and then rested at 80°C for 30, 60 and 120 minutes, which are the periods needed to give cyclic stressing up to 500, 1000 and 2000 cycles, the total tensile strains ε_t were all found to be equal to ε_0. Hence, the vacancy lifetime at 80°C is very long and is of the order of a hundred minutes in this alloy.

It is shown that Eq. (21b) is satisfied experimentally in Fig. 12, where $m+\beta=2.50$ and $m=1.50$ (hence $\beta=1.0$), which were determined from the experiment of the P-L effect in tensile deformation of the same alloy[51,52]. The strain exponent of the vacancy production during the cyclic stressing, $m_f\simeq 1.55$, was determined from the slope, and the fraction of constants, $B_f/B\simeq 1/250$, was also calculated from Eq. (21b). It becomes evident from the present results that the efficiency of the vacancy production during cyclic stressing conducted at a constant stress amplitude, is extremely lower than that during unidirectional deformation.

In each half cycle, the strain amplitude $\Delta\varepsilon$ is equivalent to the Bauschinger strain β_1 produced by the same stress as the pre-stress level. The Bauschinger strain has been attributed to the relaxation of dislocations formed by the pre-strain. Furthermore, it is believed that the dislocation density doesnot increase in this an-elestic

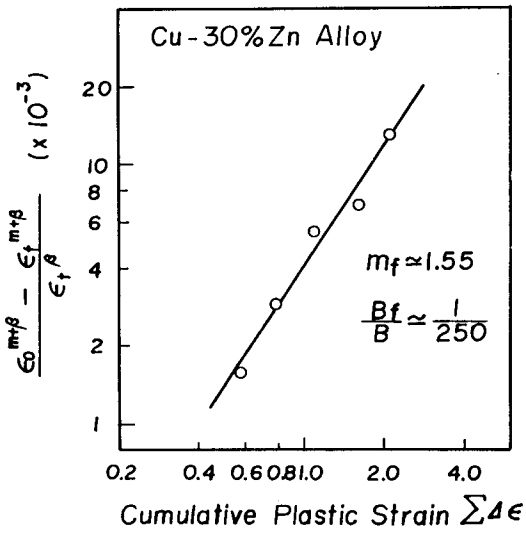

Fig. 12. Plot of the results in a form for Eq. (5b).

strain region[54,55]. Therefore, it is reasonable to consider that the loop width will be produced by the result of the to-and-fro motion of piled-up dislocations in such a metal having a lower stacking fault energy as α-brass. The non-conservative motion of jogs on screw dislocations is generally accepted for the mechanism for the formation of point defects. Accepting this mechanism for the formation of vacancies in fatigue deformation, it may be suggested that the jogs scarcely move in the anelastic strain region during fatigue at the constant stress amplitude. That is to say, the loop width is presumably accommodated with moving dislocations which bow between the jogs or other obstacles.

4. 3. 3. Dependence of strain amplitude on the onset of serration during cyclic straining

a) α-brass

From the results obtained in the previous Section 4. 3. 2, it may be suggested that during the fatigue deformation with a constant plastic strain amplitude, the efficiency of the vacancy production would decrease with an increase in the number of cycles. It may also be suggested that the concentration of vacancies would be larger for a larger strain amplitude. This because a fraction of the anelastic strain region (the Bauschinger strain region) which is occupied in a prescribed strain amplitude increases with an increase in the number of cycles. Also, this fraction is greater when the prescribed strain amplitude is smaller, as shown in a later figure.

The cyclic deformations were performed at various prescribed plastic strain amplitudes ranging from 0. 58 to 2. 05%, in order to investigate the characteristics of the occurrence of the P-L effect, and to obtain information on the vacancy production during low cycle fatigue. The deformation temperature was 80 ± 1°C, and the strain rate employed was 5.2×10^{-4}/sec.

Typical load-elongation loops, which were controlled under a constant plastic strain amplitude, are shown in Fig. 13. In the figure, part (a) is the initial $1\frac{1}{4}$ cycles, (b) is after the cycles, which was magnified five times in a load scale and an arrow indicates the onset of serration.

It appeared that a great number of cycles was necessary for the onset of serration for the lower strain amplitudes. Besides, cumulative plastic strains to the onset of serration $\Sigma\Delta\varepsilon_o$ were larger for the lower strain amplitudes, as shown in Table 4. However, the values denoted as $\Sigma\Delta\varepsilon_o-\Sigma\beta_1$, which are little larger than the critical strain for the onset of the P-L effect in the tensile deformation, ε_o by an amount of 22%, give an approximately constant amount of strain independent of the strain amplitude. In the table, the value denoted as $\Sigma\Delta\varepsilon_o-\Sigma\beta_{3/4}$ is shown for each specimen, since the Bauschinger strain $\beta_{3/4}$ is often assessed as a parameter of the

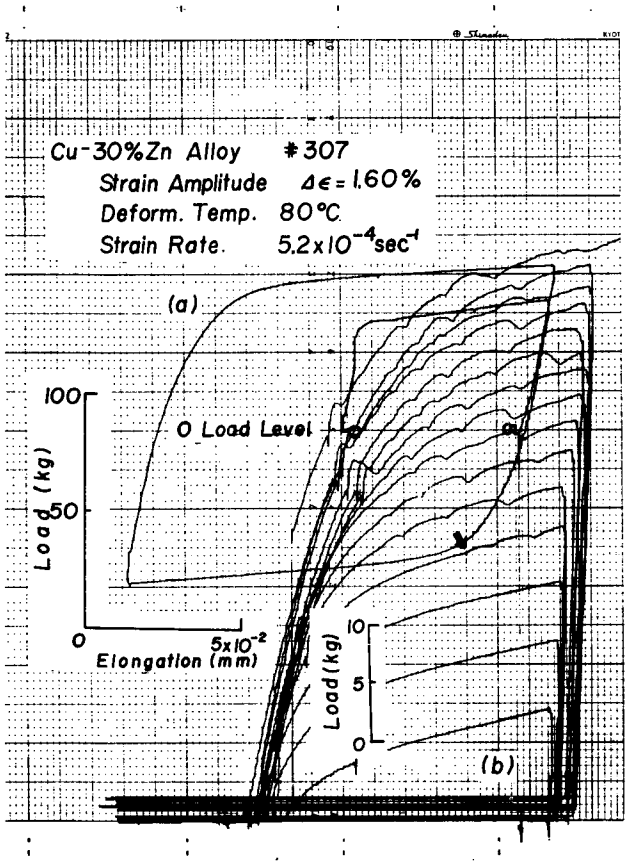

Fig. 13. Hysteresis loops showing the P-L effect in polycrystalline α-brass. Part (a) is initial 1¼ cycles, and (b) is after the cycles magnified by five times in load scale.

Table 4. Dependence of plastic strain amplitude on the onset of serration in α-brass.

Specimen No.	$\Delta\varepsilon$ (%)	$\Sigma\Delta\varepsilon_o$ (%)	$\Sigma\Delta\varepsilon_o - \Sigma\beta_{3/4}$ (%)	$\Sigma\Delta\varepsilon_o - \Sigma\beta_1$ (%)	$\sigma_o{}^c$ (kg/mm²)
#1011	2.05	10.60	9.75	6.70	10.37
# 423	1.65	14.20	12.75	7.85	9.90
# 408	1.10	22.20	18.90	7.46	9.94
# 421	0.82	23.20	19.39	7.01	10.23
# 301	0.58	29.30	22.02	6.49	10.63

Critical strain in tensile deformation: $\varepsilon_o = 5.82\%$

Critical stress in tensile deformation: $\sigma_o = 10.42$ kg/mm²

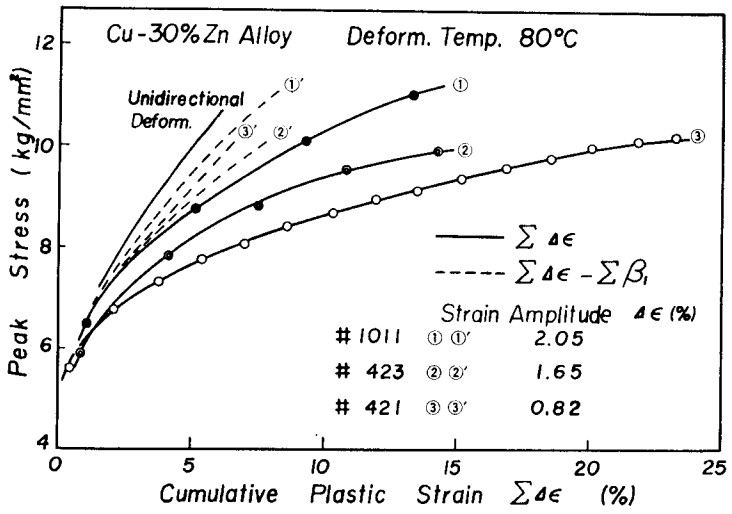

Fig. 14. Cumulative stress-strain curves for cyclic straining at various strain amplitudes in α-brass.

Bauschinger effect, but these value increase for lower strain amplitudes. The critical stress for the onset of serration during cyclic straining σ_o is also indicated. These are independent of strain amplitude and approximately equal to that for unidirectional deformation.

The relation between the peak stress of a tensile half cycle and a cumulative plastic strain, the so-called cyclic strain hardening curve, is shown in Fig. 14. Here, a unidirectional deformation curve is also indicated. The dotted lines show the results by subtracting the measured Bauschinger strain β_1. It is found that the curves in terms of $\Sigma\Delta\varepsilon-\Sigma\beta_1$ are independent of the strain amplitude and these are below the unidirectional deformation curve. It is an important fact that the Bauschinger strain β_1 is the most suitable perameter to consider the cyclic strain hardening at various strain amplitudes. In addition, the results may be interpreted to mean that the reverse strain produces a rearrangement of dislocations or an amount of annihilation of dislocations. The effect due to the reverse straining leads to the lower strain hardening in the following plastic strain region of each half cycle.

The variation of the absolute Bauschinger strain, β_n in each compressive half cycle against the cumulative strain for a specimen conducted under a high and low strain amplitude is shown in Fig. 15. The result points out that the absolute Bauschinger strain is larger for a higher strain amplitude, but the ratio denoted as $\beta_n/\Delta\varepsilon$ is larger for a lower strain amplitude, as shown in Fig. 16. This indicates that the fraction of the Bauschinger strain to the prescribed strain amplitude is greater for a lower strain amplitude.

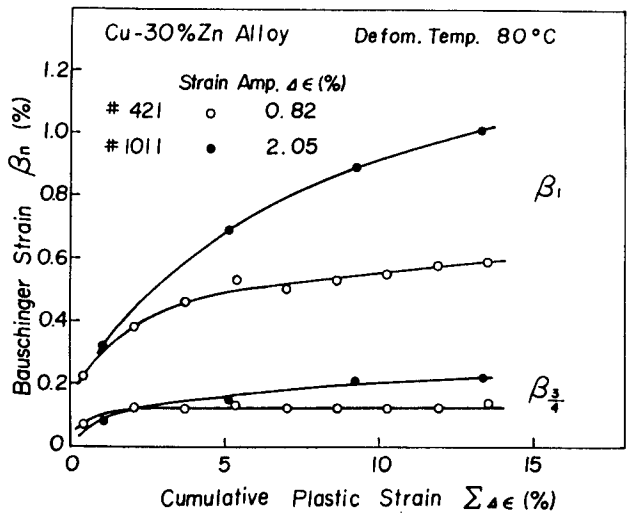

Fig. 15. Variation of Bauschinger strain β_1, $\beta_{3/4}$, with cumulative plastic strain in α-brass.

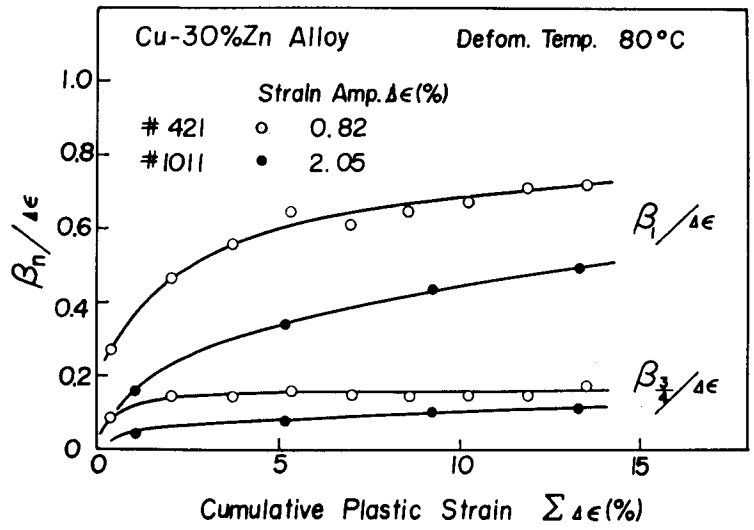

Fig. 16. Variation of the ratio $\beta_1/\Delta\varepsilon$, $\beta_{3/4}/\Delta\varepsilon$, with cumulative plastic strain in α-brass.

The results obtained previously in Section 4. 3. 1. and 4. 3. 2. indicate that the vacancies can be scarecely produced in the anelastic or the Bauschinger strain region during the reverse flow. Therefore, it may be consistent to say that a great number of cycles as well as the large value of $\Sigma\Delta\varepsilon_0$ are necessary at the start of the P-L effect for a specimen conduced with a relatively low strain amplitude. Also, the

values of $\Sigma\Delta\varepsilon_0$-$\Sigma\beta_1$ are nearly constant for the different strain amplitudes.

The most satisfactory model available to account for the production of point defects, in view of its quantitative agreement with the experimental results in fcc metals, is Saada's model[56]. It predicts that the point defect concentration produced is proportional to the work done by the plastic deformation[57-60]. The work done until the first serration occurred was measured by hysteresis loops. It was found that the cumulative works, exclusive of the Bauschinger strain region at various strain amplitudes, assuming that the point defects are not created in this region, were indipendent of the strain amplitudes and estimated to be 0.54 kgmm/mm^3. The critical work done in unidirectional deformation was 0.48 kgmm/mm^3.

b) Ag-6.3 at. % Al

A similar type of experiment to that for α-brass was performed in Ag-6.3 at. % Al polycrystals. The deformation temperatures were 20 and 40°C, and the strain rate employed was 5.4×10^{-4}/sec. The critical strain for the onset of serration was

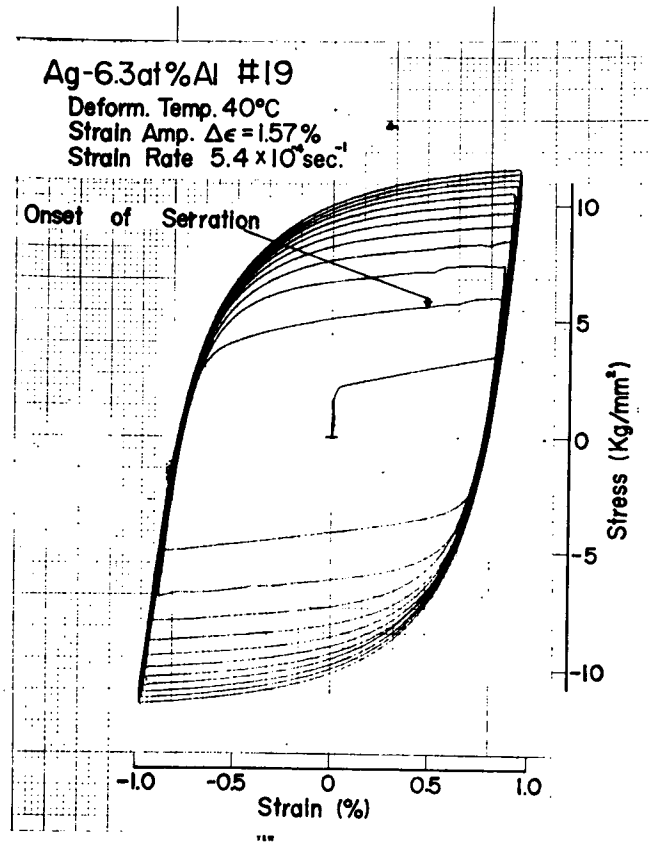

Fig. 17. Typical hysteresis loops showing the appearance of the P-L effect in Ag-6.3 at.% Al. The serration disappears at the 5th cycle.

5.08% at 20°C and 2.23% at 40°C respectively. The cyclic tension-compression tests were conducted under the prescribed strain amplitudes ranging from 0.63 to 1.76%.

Typical hysteresis loops are represented in Fig. 17. It is seen that the serrated yielding occurred at the second cycle and disappeared beyond the 5th cycle. The serration which occurred in the specimen unidirectionally deformed did not disappear at all until fracture. Thus, the disappearance observed in the present test is considered to be a specific character of cyclic straining. It was observed that with a lower strain amplitude and a lower temperature, the disappearance occurred in a low number of cycles. However, the detailed mechanism is not clear.

The critical cumulative strains for the onset of serration in cyclic deformation at various strain amplitudes are shown in Table 5. It can be clearly understood that the results are similar to those for α-brass. Although the cumulative plastic strain for the onset of serration is larger for a smaller strain amplitude, the values denoted

Table 5. Dependence of plastic strain amplitude on the onset of serration in Ag-6.3 at.% Al.

Deform. Temp.	Speci. No.	$\Delta\varepsilon$ (%)	$\Sigma\Delta\varepsilon_0$ (%)	$\Sigma\Delta\varepsilon_0-\Sigma\beta_1$ (%)	σ_0 (kg/mm²)
20°C	10	1.29	8.82	5.09	8.61
	7	1.64	7.20	5.15	8.09
40°C	35	0.63	4.64	2.73	5.69
	15	1.15	4.19	2.75	6.36
	19	1.57	3.51	2.72	5.70
	22	1.76	3.22	2.54	6.44

Mean critical strain, ε_0, and stress, σ_0, in tensile deformation: $\varepsilon_0=5.08\%$, $\sigma_0=7.73$ kg/mm² at 20°C; $\varepsilon_0=2.23\%$, $\sigma_0=5.58$ kg/mm² at 40°C

Table 6. Critical deformation energy per unit volume for the onset of serration in Ag-6.3 at.% Al.

(kgmm/mm³)

Deform. Temp.	Speci. No.	$\Delta\varepsilon$ (%)	ΣE_0	ΣE_{β_1}	$\Sigma E_0-\Sigma E_{\beta_1}$
20°C	10	1.29	0.531	0.224	0.307
	7	1.64	0.371	0.107	0.264
40°C	35	0.63	0.182	0.071	0.264
	15	1.15	0.172	0.061	0.111
	19	1.57	0.140	0.029	0.111
	22	1.76	0.150	0.029	0.121

Mean critical deformation energy in tensile deformation: $E_0=0.224$ at 20°C; $E_0=0.089$ at 40°C

as $\Sigma\Delta\varepsilon_o$-$\Sigma\beta_1$ give an approximately constant amount of strain. It is a little larger than the critical strain in the unidirectional deformation, ε_o by an amount of 20%, independent of the strain amplitude. The work done until the first serration occurred isa lso shown in Table 6. The critical cummulative works exclusive of the Bauschinger strain region, ΣE_o-ΣE_{β_1}, at various strain amplitudes gave an approximately constant value. The works for both deformation temperatures are greater than the critical works in a unidirectional deformation by about 25%.

4.4. Production of vacancies in cyclic deformation

It can be concluded that the P-L effect of the present alloys can be attributed to the interaction of mobile dislocations and moving solute atoms, under the condition that the diffusion rate of the solute atom is enchanced by a non-equilibrium vacancy concentration produced by deformation. Also, the first serration occurs when $\rho_m \cdot C_v$ reaches a certain critical value, as mentioned above. Vingsbo et al. [61] have reported that in the fatigue deformation of an α-iron, the relation between the stress σ, and the dislocation density ρ, can be represented as

$$\sigma=\sigma_f+\alpha\mu b\sqrt{\rho} \tag{22}$$

were σ_f and α are constants. Thus, assuming that when the flow stresses are equal both in unidirectional and cyclic deformations, the mobile dislocation density will also be the same in these different deformation modes for the start of the P-L effect. It appreared that the concentration of vacancies were equal for the different strain amplitudes or deformation modes, because the critical stresses for the onset of the P-L effect were approximately equal, independent of the strain amplitudes or deformation modes, as shown in Tables 4 and 5.

The results obtained previously in Section 4.3.1. and 4.3.2. indicate that the Bauschinger strain β_1 does not create vacancies. Therefore, it may be concluded that vacancies are created in a complete plastic strain region of each half cycle during cyclic deformation, which is nearly equal to a deduction of β_1 from the prescribed plastic strain amplitude. However, the efficiency of the vacancy production in this complete plastic strain region will be about 20% lower compared with that of the unidirectional deformation. This will occur when we also accept that the vacancy production by the strain is represented by the relation $C_v=B\varepsilon^m$ during cyclic straining, since $\Sigma\Delta\varepsilon_o$-$\Sigma\beta_1$ is larger than ε_o by an amount of 20% in both alloys. A similar conclusion can be derived from the measurements of work done until the first serration occurred, as pointed out in Section 4.3.3. It seems therefore that vacancies produced in a half cycle will be annihilated by an amount of 20% during the subsequent half cycles due to a vacancy-interstitial annihilation.

It has long been believed that fatigue deformation creates a large concentration of point defects in alloy too, and these facts were reviewed briefly by Dawson[53]. In

his paper, he showed that in the per unit of deformation energy, fewer point defects were produced during fatigue than in a unidirectional deformation, except perhaps during the first few cycles of cyclic stressing, using the available data of Johnson and Johnson[18] from the measurement of electrical resistivity on high-purity copper during tension-compression fatigue and unidirectional deformation.

Recently, it has been reported by Ceresara[62] that in torsion fatigue experiments of aluminium, the resistivity increases rapidly at the first cycles, and then it slows down and reaches a saturation value. It was pointed out that the saturation trend of resistivity can be correlated to the saturation in hardening, usually in metals in the initial stage of fatigue. Similar results using resistivity measurements on fatigue induced defects in fcc pure metals have been obtained[63-65]; i. e. during unidirectional deformation the resistivity increases continually, while during fatigue with a constant strain amplitude, it increases and saturates at a level which is higher for larger amplitudes.

These trends obtained by resistivity measurements are consistent with the present results, predicting that during cyclic straining the efficiency of the vacancy production would decrease with an increase in the number of cycles. Also, the saturation of vacancy production is directly correlated to the saturation of cyclic strain hardening. It is worth while nothing that the consideration of the Bauschinger strain in each cycle is inevitable for any discussion about the efficiency of vacancy

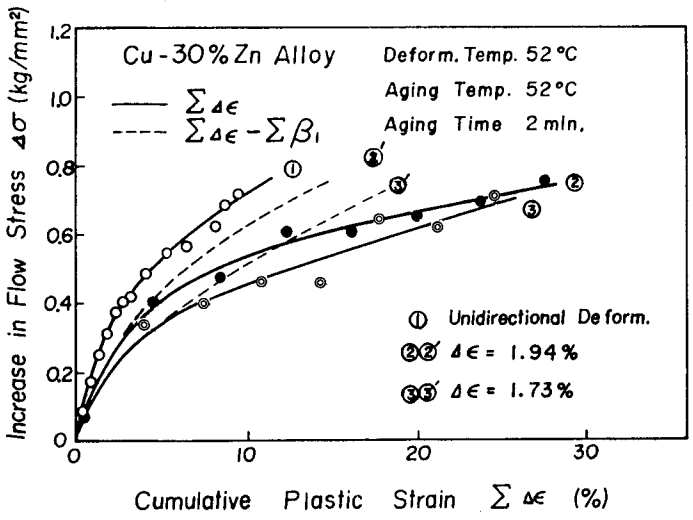

Fig. 18. Relation between the increase in flow stress due to static strain aging and the cumulative strain in cyclic deformation of α-brass. Increase in flow stress in unidirectional deformation is also indicated and dotted lines show the results of subtractions of the cumulative Bauschinger strain.

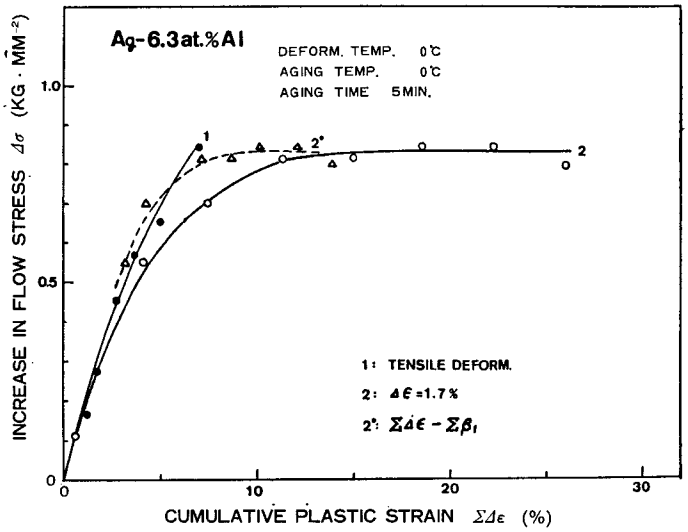

Fig. 19. Relation between the increase in flow stress due to static strain aging and the cumulative strain in cyclic deformation of Ag-6.3 at.% Al.

production to cyclic straining.

It is shown in Section 4.2.3. that the increase in flow stress in static strain aging is strongly affected by the accumulation of vacancies produced by strain. In cyclic deformation, static strain aging experiments were performed in order to test the prediction about the vacancy production during fatigue. Increases in flow stress against cumulative strains for α-brass and Ag-Al are plotted, as shown in Figs. 18 and 19 respectively. It can be easily understood from the results that the prediction is almost satisfied.

However, it has been reported that the initial efficiency of point defects production during fatigue can be larger than that in unidirectional deformation of pure aluminium, gold[63], and copper[53]. In the present results, on the contrary, the efficiency during fatigue is always smaller than that during unidirectional deformation. This difference may be due to a difference in the movement of dislocations under a reverse stress related to the stacking fault energy of metals.

5. Conclusions

In order to investigate the characteristics of the P-L effect, and to obtain additional information on the production of vacancies during tensile and fatigue deformation, tensile and tension-compression tests were performed in Ag-6.3 at.% Al and α-brass polycrystals. The main results can be summarized as follows:

1) The P-L effect of Type A in Ag-Al alloy is well explained by the dynamic strain aging (Cottrell) model. The critical strain for the onset of serration ε_0 and

the strain rate $\dot{\varepsilon}$ are related as $\dot{\varepsilon} \propto \varepsilon_0^{2.5}$.

2) The activation energy for the migration of a vacancy in Ag-Al alloy is estimated to be 0.60 ± 0.02 eV, which is considered to the migration energy of a vacancy which was bound with a Al atom.

3) The P-L effect of Ag-Al alloy is strongly affected by the accumulation of vacancies produced by strain. From the experiment of annealing out the excess vacancies (pre-strain experiment), the strain exponent m of the vacancy concentration produced by strain was determined to be $m=1.35$.

4) The exponent m was also determined by the experiment of static strain aging, and the obtained value was equal to that of the pre-strain experiment, assuming the strain exponent of total dislocation density $\beta=1$.

5) From the cyclic stressing test and the measurements of the subsequent strain for the onset of the P-L effect, it was concluded that vacancies are scarcely produced during a cyclic deformation at a constant stress amplitude.

6) In the cyclic straining conducted under the prescribed strain amplitude, cumulative strain to the onset of the P-L effect is greater for a lower strain amplitude. However, the values subtracted by the Bauschinger strains from the cumulative strains give an approximately constant value independent of the strain amplitude. Also, the values are larger than the critical strain for unidirectional deformation by about 20% in both alloys.

7) From the characteristics of the P-L effect, it can be concluded that vacancies are produced only in the complete plastic strain region subsequent to the Bauschinger strain β_1 in during cyclic straining. Therefore, the efficiency of vacancy production would decrease with an increase in the number of cycles; i. e., the saturation of vacancy production is to be directly correlated to the saturation of cyclic strain hardening.

8) The efficiency of vacancy production during cyclic straining is lower by 20% even in the complete plastic strain region. This may be caused by the vacancy-interstitial annihilation.

References

1) A. Portevin and F. Le Chatelier; Compt. Rend. Acad. Sc., **176**, 507 (1923).
2) See for a review, B. J. Brindley and P. J. Worthington; Met. Rev., **145**, 101 (1970).
3) J. D. Baird; The Inhomogeneity of Plastic Deformation, Amer. Soc. Met., p. 191 (1972).
4) S. Miura, J. Takamura and N. Nagata; Suiyōkai-shi, Kyoto Univ., **15**, 216 (1964).
5) Y. Bergström and W. Roberts; Acta Met., **19**, 815 (1971).
6) S. Miura; Mechanical Behavior of Materials, Soc.. Mater. Sci. Japan, Vol. 1, p. 128(1972).
7) N. Thompson and N. J. Wadsworth; Adv. Phys., **7**, 72 (1958).
8) A. M. Adair and H. A. Lipsitt; Trans. AIME, **236**, 1235 (1966).
9) G. Oates and D. V. Wilson; Acta Met., **12**, 21 (1964).
10) D. V. Wilson; Phil. Mag., **22**, 643 (1970).

11) D. V. Wilson and J. K. Tromans; Acta Met., **18**, 1197 (1970).
12) D. V. Wilson; Proc. 3rd. Int. Conf. Strength of Metals and Alloys, Vol. 1, 417 (1973).
13) J. C. Swearengen, R. Taggart and H. I. Dawson; Scripta Met., **4**, 637 (1970).
14) S. Miura and S. Hashimoto; Scripta Met., **6**, 667 (1972), Ibid., **6**, 673 (1972).
15) S. Hashimoto and S. Miura; Mechanical Behavior of Materials, Soc. Mater. Sci. Japan, Vol. II, p. 31 (1974).
16) W. Wagner and E. Macherauch; Z. Metallkde., **65**, 123 (1974).
17) H. M. Rosenberg; Vacancies and Other Point Defects in Metals and Alloys, Institute of Metals, London, 829 (1958).
18) E. W. Johnson and H. H. Johnson; Trans. AIME, **233**, 1332 (1965).
19) A. H. Cottrell; Phil. Mag., **44**, 829 (1953).
20) A. H. Cottrell; Vacancies and Other Point Defects in Metals and Alloys, Inst. Met., p. 1 (1958).
21) B. Russell; Phil. Mag., **8**, 615 (1963).
22) R. K. Ham and D. Jaffrey; Phil. Mag., **15**, 247 (1967).
23) See for example, J. Friedel; Dislocations, Pergamon, p. 84 (1964).
24) F. Seitz; Adv. Phys., **1**, 43 (1952).
25) N. F. Mott; Phil. Mag., **43**, 1151 (1952).
26) K. L. Murty, F. A. Mohamed and J. E. Dorn; Scripta Met., **5**, 1087 (1971).
27) P. G. McCormick and K. L. Murty; Scripta Met., **6**, 225 (1972).
28) S. R. MacEwen and B. Ramaswani; Phil. Mag., **22**, 1025 (1970).
29) H. G. Van Bueren; Acta Met., **3**, 519 (1955).; Z. Metallkde., **46**, 272 (1955).
30) N. F. Mott; Phil. Mag., **44**, 187, 742 (1953).
31) H. G. Van Bueren; Imperfections in Crystals, North-Holland (1960).
32) J. Takamura; Physical Metallurgy, edited by R. W. Cahn, North-Holland, p. 714 (1965).
33) W. G. Johnston and J. J. Gilman; J. Appl. Phys., **30**, 129 (1959).
34) A. H. Cottrell and B. A. Bilby; Proc. Phys. Soc., **62A**, 49 (1949).
35) S. Harper; Phys. Rev., **83**, 709 (1951).
36) G. F. Bolling; Phil. Mag., **4**, 537 (1959).
37) A. A. Hendrickson and M. E. Fine; Trans. AIME, **221**, 103 (1961).
38) S. Miura and H. Kawano; Japan Inst. Light Metals, **21**, 358 (1971).
39) S. G. Gertsriken and N. N. Nowikow; Fis Metallow i Metallowedenie, **9**, 224 (1960).
40) W. Schule, A. Seeger, F. Ramsteiner, D. Schulemacher and K. King; Z. Naturfosch., **15a**, 323 (1961).
41) M. Doyama and J. S. Koehler; Phys. Rev., **119**, 939 (1960); **127**, 21 (1962).
42) H. I. Dawson; Acta Met., **13**, 453 (1965).
43) Y. Qnere; J. Phys. Soc. Japan, **18**, Suppl. III, 91 (1963).
44) F. Cattaneo and E. Germagnoli; Phys. Rev., **124**, 414 (1961).
45) L. J. Cuddy and E. S. Machlin; Phil. Mag., **7**, 745 (1962).
46) A. J. R. Soler-Gomez and W. J. McG. Tegart; Phil. Mag., **20**, 495 (1969).
47) B. Russell and P. Vela; Phil. Mag., **8**, 677 (1963).
48) T. E. Mitchell; Prog. Appl. Mat. Res., **6**, 117 (1964).
49) J. D. Livingston; Acta Met., **10**, 229 (1962).
50) J. J. Gilman; Micromechanics of Flow in Solids, McGraw-Hill, p. 190 (1969).
51) S. Miura and S. Matsuba; Pre-print, the Meeting of Japan Inst. Metals, Oct., p. 67 (1970).
52) S. Miura and S. Kubo; Pre-print, the Meeting of Soc. Mater. Sci. Japan, May, p. 233 (1972).
53) H. I. Dawson; J. Appl. Phys., **39**, 3022 (1968).
54) S. Hashimoto, S. Miura and T. Yagi; Scripta Met., **10**, 823 (1976).
55) S. Hashimoto and S. Miura; Proc. ICSMA 4, 65 (1976).

56) G. Saada; Physica, **27**, 657 (1961).
57) A. van den Beukel; Vacancies and Interstitials of Metals, eds., A. Seeger ea al., North-Holland, p. 427 (1969).
58) A. van den Beukel; Acta Met., **11**, 97 (1963).
59) H. I. Dawson; Physica, **31**, 342 (1965).
60) S. Ceresara, H. Elkholy and T. Federighi; Phys. Stat. Sol., **8**, 509 (1965).
61) O. Vingsbo, Y. Bergström and G. Largerberg; Phil. Mag., **19**, 1271 (1969).
62) S. Cerasara; Phil. Mag., **19**, 99 (1969).
63) S. R. Mitchell and H. I. Dawson; Met. Trans., **1**, 1205 (1970).
64) R. G. Baggerly and H. E. Dawson; Scripta Met., **5**, 319 (1971).
65) S. J. Goldberg, R. J. Maciag and K. Mukherjee; Met. Trans., **1**, 1079 (1970).